Coupling scheme for complete synchronization of periodically forced chaotic CO_2 lasers

I. P. Mariño,[1,2] E. Allaria,[3] M. A. F. Sanjuán,[1] R. Meucci,[2] and F. T. Arecchi[2,3]

[1]*Nonlinear Dynamics and Chaos Group, Departamento de Matemáticas y Física Aplicadas y Ciencias de la Naturaleza,*
Universidad Rey Juan Carlos, Tulipán s/n, 28933 Móstoles, Madrid, Spain
[2]*Istituto Nazionale di Ottica Applicata, Largo E. Fermi 6, 50125 Firenze, Italy*
[3]*Department of Physics, University of Florence, Firenze, Italy*

We present a way of coupling two nonautonomous, periodically forced, chaotic CO_2 lasers in a master-slave configuration in order to achieve complete synchronization. The method consists of modulating the forcing of the slave laser by means of the difference between the intensities of the two lasers, and lends itself to a simple physical implementation. Experimental evidence of complete synchronization induced by a suitable coupling strength is shown, and a numerical model is used to achieve further insight of the synchronization phenomena. Finally, we describe a possible application of the investigated technique to the design of a digital communication system.

I. INTRODUCTION

Chaotic synchronization is of fundamental importance in a variety of complex physical, chemical, biological, and ecological systems [1–5]. When two chaotic systems interact, different synchronization regimes can be obtained, including complete or identical synchronization [1,6,7], lag synchronization [8], phase synchronization [9], and generalized synchronization [10,11]. These synchronization regimes have been described theoretically and observed experimentally in many different systems, some of them reviewed in Ref. [3]. Among the different systems where synchronization has been achieved, lasers are of particular interest, due to the potential applications to secure optical communications [12,13].

Synchronization has been usually studied for autonomous chaotic systems, that is, systems which are not subject to an external time-dependent driving. In this situation a coupling between two or more systems (identical or not) can induce changes in some properties of the dynamics of the systems, giving rise to a common behavior.

Here, we focus our attention on the synchronization of coupled nonautonomous chaotic systems, where the chaotic behavior of each system is a consequence of an external periodic forcing. A theoretical investigation on this problem for the case of the forced Van der Pol oscillator can be found in Ref. [14]. Experimental works on modulated lasers where the coupling is carried out by a superposition of the two electric fields with a common laser medium have also been reported [15–18].

In this work, we consider the connection of two chaotic lasers in a master-slave configuration that are coupled by modulating the amplitude of the external forcing of the slave laser. The introduction of this new coupling scheme is the main contribution of this paper. The control signal to be used for modulating the amplitude of the external forcing signal in the slave laser is obtained as the difference between the intensities of the two lasers. This difference must go to zero in the synchronized regime [6,19]. This technique is simple to implement in most practical setups and can be easily ex-

tended to other systems with external periodic forcing.

The paper is organized as follows. Section II describes the experimental setup including the details of the implementation of the proposed coupling method. A numerical model that accurately reproduces the experimental behavior is presented in Sec. III. Both experimental and numerical results that characterize the synchronization phenomenon are presented and analyzed in Sec. IV. Section V is devoted to a simple application example in the field of digital communications, and concluding remarks are made in Sec. VI.

II. EXPERIMENTAL SETUP

In order to experimentally investigate the synchronization between two CO_2 lasers in a master-slave configuration, we have designed the experimental setup shown in Fig. 1. The laser cavity is defined by a totally reflecting grating and a partially reflecting mirror (R and $M2$), and the gain medium is pumped by an electric discharge current of 6 mA. An electrooptic modulator (EOM) is inserted in the laser cavity in order to control the cavity losses by an external forcing ob-
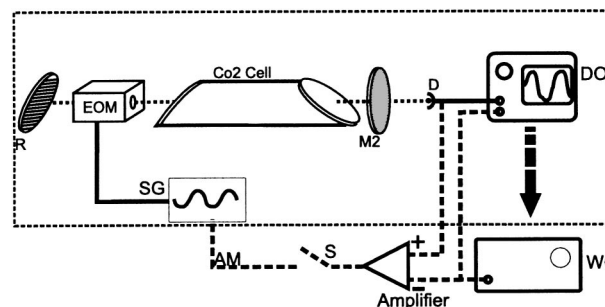

FIG. 1. Experimental setup for a CO_2 laser with modulated losses. EOM: intracavity electrooptic modulator, R: total reflecting grating, $M2$: partial reflecting mirror, D: fast infrared detector, SG: sinusoidal generator, DO: digital oscilloscope, S: switch, WG: arbitrary wave-form generator which can reproduce a wave form previously acquired with DO.
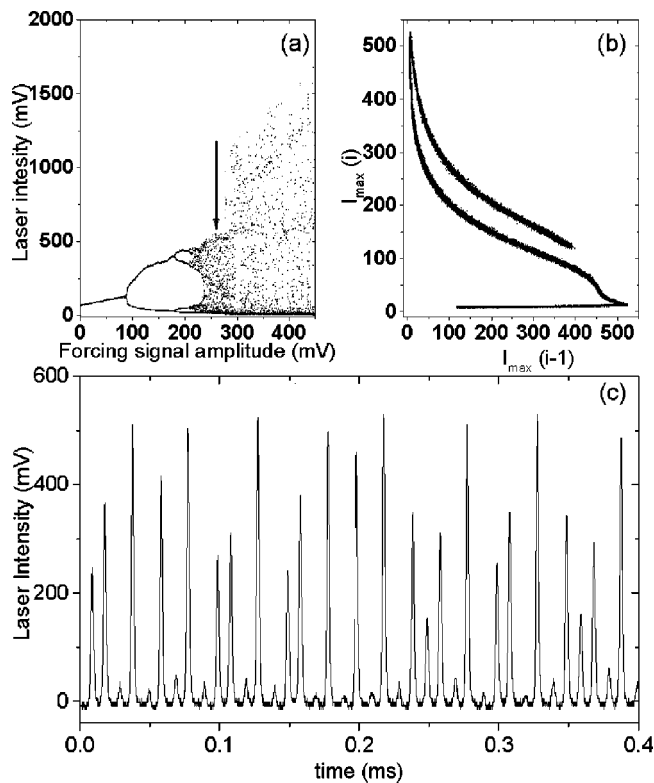
FIG. 2. (a) Experimental characteristic bifurcation diagram for the CO_2 laser with modulated losses as a function of the amplitude of the external forcing. The arrow indicates the region where our laser is set. (b) Return map of the laser intensity showing a chaotic attractor. (c) Experimental temporal evolution of the laser intensity, showing uniform phase evolution with chaotic amplitudes, which take values in the interval (0, 550) mV.

tained from a sinusoidal generator (SG). Such a signal has a frequency of $f_{sin}=100$ kHz, which is around the double of the relaxation frequency of the laser. By increasing the driving amplitude of the external periodic forcing signal, the system displays a transition to chaos through a sequence of subharmonic bifurcations [see Fig. 2(a)]. A further increase of this amplitude, which plays the role of our control parameter, leads the system to an interior crisis [23] characterized by a widening of the chaotic attractor, as shown in the bifurcation diagram in Fig. 2(a). In the experiment, we set the system in the chaotic region before the occurrence of the interior crisis, as indicated by the arrow in Fig. 2(a). A return map of the laser intensity of this chaotic state is represented in Fig. 2(b), where a chaotic attractor is shown. The temporal evolution of the laser intensity is plotted in Fig. 2(c), to show that the frequency of the spikes is constant while the amplitudes are chaotic. This particular behavior, not so typical in physical systems, was previously described in Ref. [24] as uniform phase evolution with chaotic amplitudes in relation to some synchronization phenomena in a model of an ecological system.

We achieve a master-slave configuration with a single laser by an adequate use of the experimental setup of Fig. 1. Specifically, a "master" signal is obtained by recording the time sequence of the laser when there is no amplitude modulation (AM) on the sinusoidal generator (i.e., the switch S is

open, so that there is no feedback in the loop of Fig. 1). A long time sequence (more than 1000 laser pulses) is stored by means of the digital oscilloscope (DO) with high time resolution (0.1 μs). In a second stage, the recorded master signal is reproduced by the wave-form generator (WG) and the feedback loop is activated. The CO_2 laser behaves now as a slave system, and coupling is achieved by using the difference between the master signal and the slave-laser intensity, amplified by a coupling factor, as an amplitude modulation applied to the sinusoidal generator of the slave laser. If the coupling factor is high enough and both systems are sufficiently close in phase, a complete synchronization regime is achieved. It is worth noting that we are considering the phases of the laser intensities and not the phases of the laser electric fields. Since we use an optoelectronic system (see Fig. 1), instead of an all-optical (coherent) system, as in Refs. [15–18], it is not necessary to match the phases of the electric fields.

The coupling scheme is a fairly general one and can be applied to a broad class of periodically forced chaotic systems. This is so because, from a dynamical point of view, by modulating the amplitude of the external periodic forcing signal we have found a very simple and experimentally realizable way of adaptively shifting the position of the slave system in its bifurcation diagram [see Fig. 2(a)]. If the modulating signal is sufficiently small, then the slight changes in the bifurcation diagram are constrained to the region of interest, where a chaotic regime with *small* amplitude and constant frequency is attained, and the slave system correctly tracks the time evolution of the master.

Driving a system with a recorded signal coming from an identical response system was also implemented in a far-infrared ammonia laser [20] and in a multimode Nd-ytrium aluminum garnet (YAG) microchip laser subjected to electrooptic feedback [21]. In both cases generalized synchronization has been demonstrated. Note, however, that the latter systems are autonomous chaotic oscillators.

III. NUMERICAL MODEL

The chaotic behavior of the previously described laser can be reproduced numerically by using the following model of five differential equations [22]:

$$\dot{x}_1 = kx_1\{x_2 - 1 - \alpha \sin^2[F(t)]\},$$

$$\dot{x}_2 = -\gamma_1 x_2 - 2kx_1x_2 + gx_3 + x_4 + p,$$

$$\dot{x}_3 = -\gamma_1 x_3 + gx_2 + x_5 + p, \quad (1)$$

$$\dot{x}_4 = -\gamma_2 x_4 + zx_2 + gx_5 + zp,$$

$$\dot{x}_5 = -\gamma_2 x_5 + zx_3 + gx_4 + zp,$$

where

$$F(t) = \beta \sin(2\pi ft + \phi_m) + b \quad (2)$$

is the external forcing signal of the master laser. In the above equations, x_1 represents the laser output intensity, x_2 is the

population inversion between the two resonant levels, and x_3, x_4, and x_5 account for molecular exchanges between the two levels resonant with the radiation field and the other rotational levels of the same vibrational band. The parameters of the model are the following: k is the unperturbed cavity loss parameter, g is a coupling constant, γ_1 and γ_2 are population relaxation rates, z accounts for an effective number of rotational levels, α accounts for the efficiency of the electrooptic modulator, and p is the pump parameter. The rest of the parameters are related to the external periodic forcing. In particular, f and ϕ_m are, respectively, the frequency and the initial phase of the external forcing, b is the bias voltage, and β is the amplitude of the external forcing. One important feature of this system is that the phase of the output intensity, x_1, is locked to the phase of the forcing signal, $F(t)$.

These equations are employed to reproduce the behavior of the master laser. Note that a simpler model, consisting of only three differential equations, is enough for a *qualitative* simulation of the laser behavior, but using the complete model (1) yields far more accurate results [25]. The set of parameters chosen to reproduce the chaotic regime is given by $k=32.97$, $\alpha=4$, $\gamma_1=10.0643$, $g=0.05$, $p=0.0198$, $\gamma_2=1.0643$, $z=10$, $\beta=0.08$, $f=1/7$, and $b=0.2$. The stability analysis provides a value of the relaxation oscillation frequency of 0.07, which is around half of the frequency of the forcing signal.

The slave laser is modeled by the same differential equations as the master laser, but adequately modifying its external sinusoidal forcing function $F(t)$. In particular, the amplitude of the external forcing function β is modulated by the intensity difference between the two lasers to yield

$$F(t) = \beta[1 + \epsilon(x_1 - y_1)]\sin(2\pi f t + \phi_s) + b, \qquad (3)$$

where y_1 and x_1 represent the output intensity of the slave and the master lasers, respectively, ϕ_s is the initial phase of the forcing signal applied to the slave laser, and ϵ represents the coupling strength between the two systems. By modulating the amplitude we move on the bifurcation diagram of the slave laser [see Fig. 2(a)] in order to correctly follow the time evolution of the master system.

The two initial phases of the forcing signals are set to zero, that is, $\phi_m = \phi_s = 0$. It has been shown that the phase difference between the external forcings plays an important role in the control of such a system [25] but, due to the complexity of the problem, it is not investigated in this manuscript and will be addressed in a future work.

IV. RESULTS

In this section we present both experimental and numerical results that illustrate the complete synchronization of the coupled nonautonomous chaotic lasers. In order to measure the degree of synchronization between the two systems, we define the following discrete-time integrated error signal

$$e_T(k) = \frac{1}{T}\int_{(k-1)T}^{kT}\left(\frac{x_1 - y_1}{\langle x_1 \rangle}\right)^2 dt, \quad k = 0, 1, \ldots, \qquad (4)$$

where k is the spike number, T is an arbitrary integration period, and $\langle x_1 \rangle$ is the mean value of variable x_1. In this case,
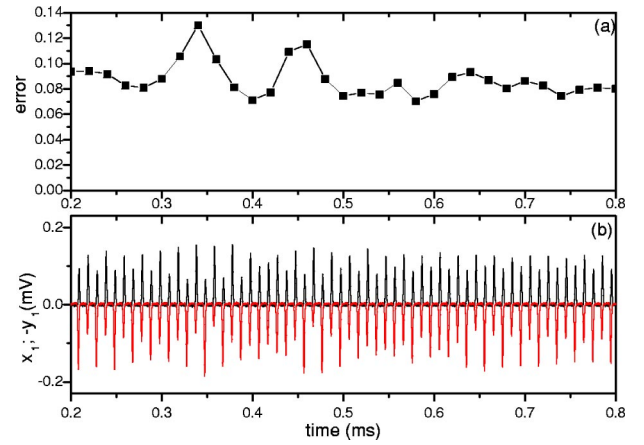

FIG. 3. Master and slave lasers when there is no coupling between them. (a) Integrated error signal defined as in Eq. (4), obtained from experimental data, and represented as a function of time. (b) Experimental temporal evolution of the output intensity of the master and the slave laser, that is, x_1 and y_1, respectively. Notice that for a better observation of the spike amplitudes, y_1 has been represented in the negative part of the vertical axis, that is, represented as $-y_1$.

a straightforward choice is to set $T=1/f_{\sin}$, where $f_{\sin}$ is the frequency of the sinusoidal signal generator employed to synthetize the external forcing functions for both the master and the slave lasers.

In order to characterize the role of coupling in synchronization, we have calculated the error signal for the uncoupled (see Fig. 3) and coupled (see Fig. 4) systems in our experiment. In Fig. 3(b), we present the temporal evolution of the master- and slave-laser intensities, x_1 and y_1, respectively. The phase of the laser intensity, in the considered setup, depends directly on the phase of the external periodic forcing. Since the phases of the forcing signals applied to the master
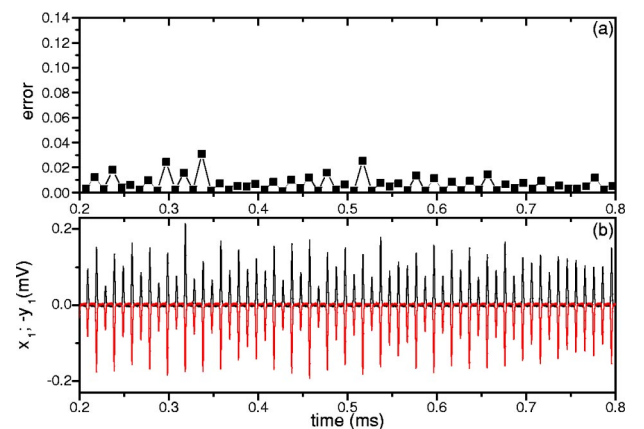

FIG. 4. Master and slave lasers when both systems are coupled. (a) Integrated error signal, obtained from experimental data, and represented as a function of time. (b) Experimental temporal evolution of the output intensity of the master laser and the slave laser, that is, x_1 and y_1, respectively. As in the previous figure, in order to obtain a better observation of the spike amplitudes, y_1 has been represented in the negative part of the vertical axis, that is, represented as $-y_1$.
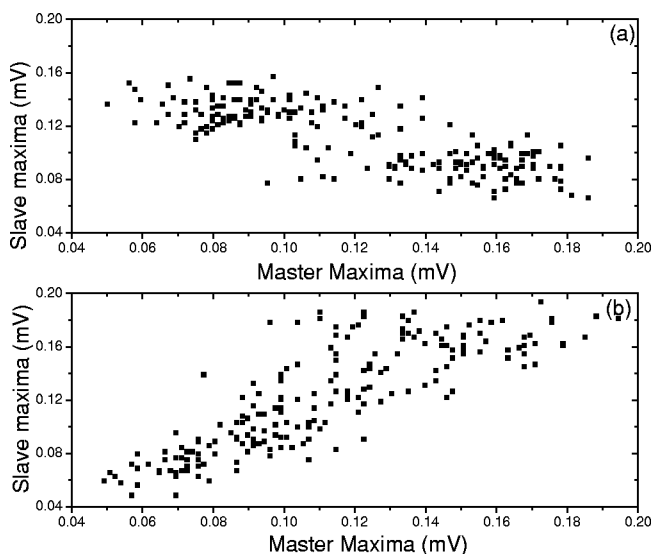
FIG. 5. Experimental correlation plots between the amplitudes of the spikes corresponding to the master and the slave lasers. (a) Uncoupled systems: the points are scattered all over the plane. (b) Coupled systems: the points are concentrated around the diagonal (with deviations due to sampling and experimental noise effects).

and the slave lasers are identical, intensities x_1 and y_1 are always in phase. Despite this phase lock, when the lasers are not coupled there is no correlation between the spike amplitudes of the two intensities and, as a consequence, the mean value of the integrated error signal in the stationary state reaches a high value, around 0.10 [see Fig. 3(a)]. If the lasers are coupled, the mean value of the integrated error diminishes considerably. In particular, for an adequate coupling strength, set by the gain of the feedback amplifier, this reduction is of one order of magnitude, that is, the mean value of $e_T(k)$ is less than 0.01 [see Fig. 4(a)]. For this situation, synchronization between the intensities of the master and the slave lasers is obtained, as seen in the temporal evolution of x_1 and y_1, represented in Fig. 4(b).

We also present the experimentally obtained correlation plots between the amplitudes of the spikes corresponding to the master and slave lasers for the uncoupled [Fig. 5(a)] and coupled [Fig. 5(b)] cases. In the former case the points are spread around the plane, whereas in the latter they are concentrated around the diagonal, indicating synchronization. The deviation from the diagonal observed in Fig. 5(b) is associated with sampling and experimental noise effects.

We have experimentally verified synchronization using the proposed scheme, but, in order to better characterize the conditions that enable synchronization and the robustness of our method, it is convenient to resort to the numerical model described in Sec. III. We pay attention first to the transient regime, that is, to what happens just after coupling the lasers. Figure 6 has been obtained numerically with a coupling factor $\epsilon=200$. We have plotted: (a) the intensity of the master-laser signal during 400 μs after the coupling, x_1; (b) the intensity of the slave-laser signal, y_1, during the same time; and (c) the resulting error signal, $e_T(k)$, during an interval of 1500 μs after the coupling. We can see how in 500 μs, the integrated error signal decreases from a value of, approxi-
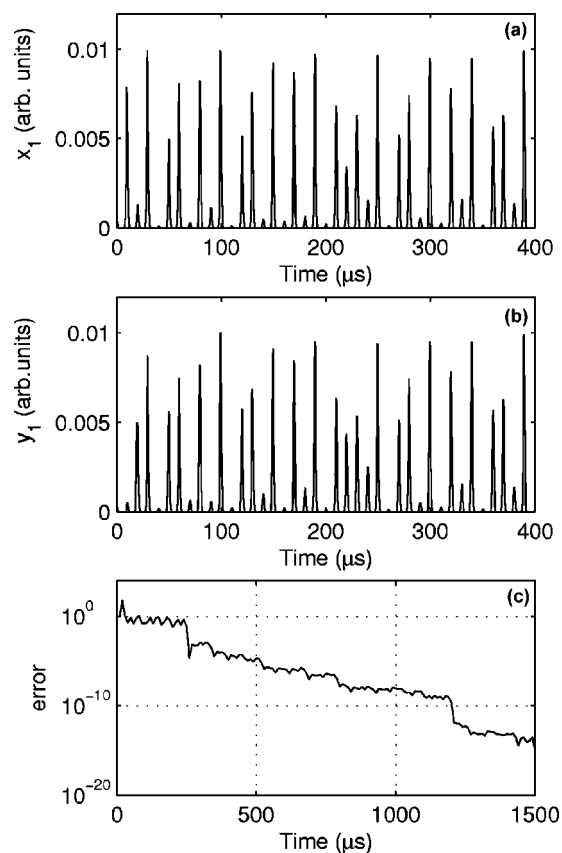

FIG. 6. Numerical example of the complete synchronization achieved between the master and the slave lasers when the coupling parameter $\epsilon=200$. (a) Temporal evolution of the output intensity of the master laser, x_1. (b) Temporal evolution of the output intensity of the slave laser, y_1. (c) Error signal defined as in Eq. (4) and represented in logarithmic scale as a function of the time.

mately, 10^0 to less than 10^{-5}. In fact, the two signals, x_1 and y_1, are practically indistinguishable after 250 μs. This is observed in Figs. 6(a) and 6(b), and corroborated by the correlation plot of Fig. 7. This plot is strictly linear, since it is free from the experimental noise effects observed in Fig. 5(b), and shows a clear evidence that complete synchronization is achieved.
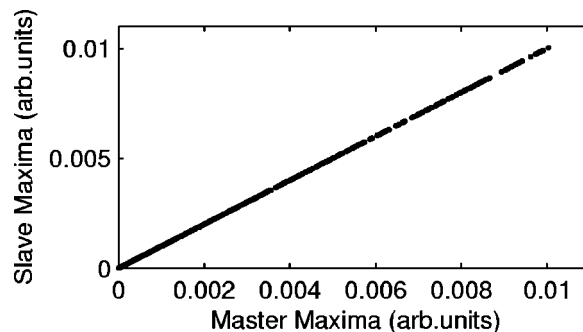

FIG. 7. Numerical correlation plot between the amplitudes of the spikes corresponding to the master and the slave lasers, after transient behavior, when the coupling parameter is $\epsilon=200$. Unlike in Fig. 5(b), a perfect diagonal is observed because numerical calculations are free from experimental noise effects and disturbances.
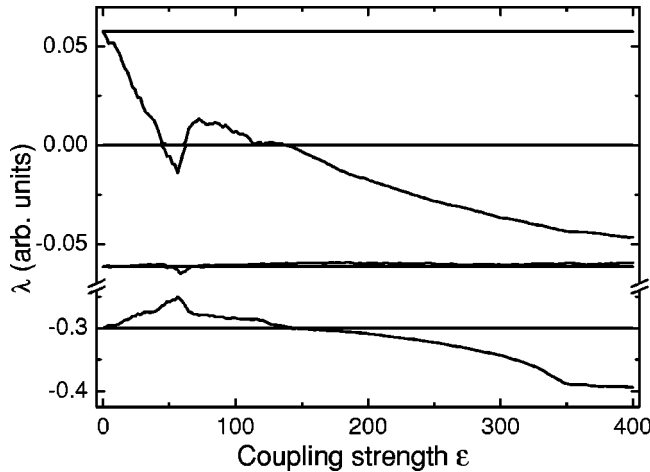
FIG. 8. Conditional Lyapunov exponents, obtained from the numerical model, as functions of the coupling strength ϵ. Note that for a certain range of parameters of the coupling strength the exponent responsible for the synchronization phenomenon moves from positive to negative values, meaning that synchronization has been achieved.

Let us consider now the dependence of the complete synchronization regime with respect to the coupling strength, controlled by the parameter ϵ in the model. This information is easily obtained by computing the conditional Lyapunov exponents of the coupled system as functions of ϵ. In Fig. 8 it is shown that the conditional Lyapunov exponent responsible for the synchronization phenomenon moves from positive to negative values as the coupling strength is increased. In particular, our study indicates that complete synchronization is achieved for $\epsilon > 160$.

A further investigation on the dependence of the synchronization behavior on the coupling parameter, ϵ, has been carried out by means of computer simulations to estimate the average time required to bring the integrated error, $e_T(k)$, below a certain threshold for a range of values of the coupling parameter where synchronization takes place, namely $\epsilon \geq 160$. For each value of ϵ, 30 simulation trials (with independently drawn random initial conditions) have been performed and the time required to attain $e_T(k) < 10^{-4}$ has been determined. The results are plotted in Fig. 9. From this figure, it is clearly observed that the average synchronization time decreases with the coupling strength, up to a value of approximately 200 μs.

Both experimental and numerical studies give evidence that the regime of complete synchronization is not affected by changes of a small percentage of the two control parameters (bias parameter, b, and pump parameter, p) on the slave laser with respect to those of the master. Therefore, to illustrate the actual robustness of our scheme, we have carried out numerical simulations to estimate the average value of the integrated error after 340 μs, that is, $e_T(k=34)$, when the bias and the pump parameters of the master laser are fixed to $b=0.2$ and $p=0.0198$, respectively, and the corresponding parameters in the slave laser are varied as represented in the horizontal axis of Figs. 10(a) and 10(b). The remaining parameters of both lasers have the values indicated in Sec. III
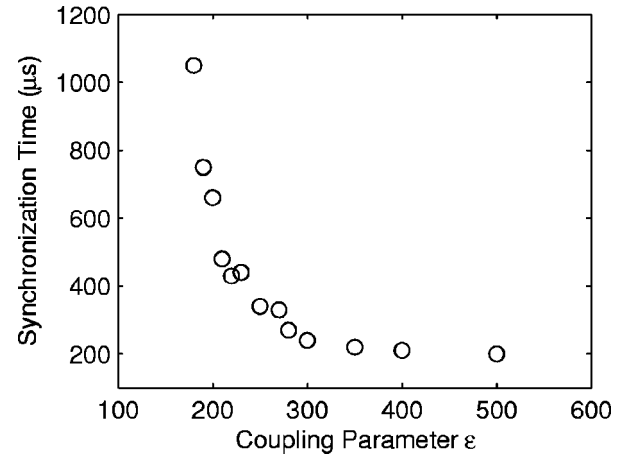

FIG. 9. Synchronization time, obtained from the numerical model, as a function of the coupling parameter ϵ. A large decrease of the synchronization time is observed, reaching a value of 200 μs for $\epsilon > 350$.

and the coupling strength is $\epsilon = 250$. We have performed 100 simulation trials with different initial conditions for each value of the slave and pump parameters in order to estimate the mean value of the integrated error $e_T(34)$, represented by circles in Figs. 10(a) and 10(b). The crosses in these plots represent the 0.9 quantile of the empirical distribution of the integrated error $e_T(34)$, i.e., the value q such that the probability of the event $e_T(34) < q$ is 0.9 according to the simulations. From this information it is deduced that the integrated error grows smoothly as the master and slave parameters diverge, but synchronization is still achieved.

V. APPLICATION TO DIGITAL COMMUNICATIONS

As an example of practical application of the synchronization properties of the investigated nonautonomous chaotic system we address the design of a simple digital transmission system, depicted in Fig. 11. We consider a message consisting of a sequence of bits "1" and "0" and let $s = x_1 m$ be the transmitted signal, where x_1 is the output intensity of the master laser and m is the information carrying signal. When a bit "0" is transmitted, $m = 1$, while $m = d \cos(2\pi t)$, with $d = 1.2$, during the transmission of a bit "1." The received signal, $s_r = s + n$, where n is a white Gaussian noise process, is used to couple the master and slave lasers through the external sinusoidal forcing function of the slave laser, that is,

$$F(t) = \beta[1 + \epsilon(s_r - y_1)]\sin(2\pi ft + \phi_s) + b, \qquad (5)$$

where ϵ is selected in the range of values that allows synchronization, as calculated from the conditional Lyapunov exponents and shown in Fig. 8. As before, we have constrained ourselves to the case in which the forcing functions of the master and the slave lasers are in phase. Recall that setting the forcing signals of the lasers in phase is equivalent to getting the corresponding intensities also in phase. Fortunately, it is simple in practice to put the received signal, s_r, in phase with the slave intensity. It is enough to use a buffer to briefly hold s_r as it is received and then release it with an
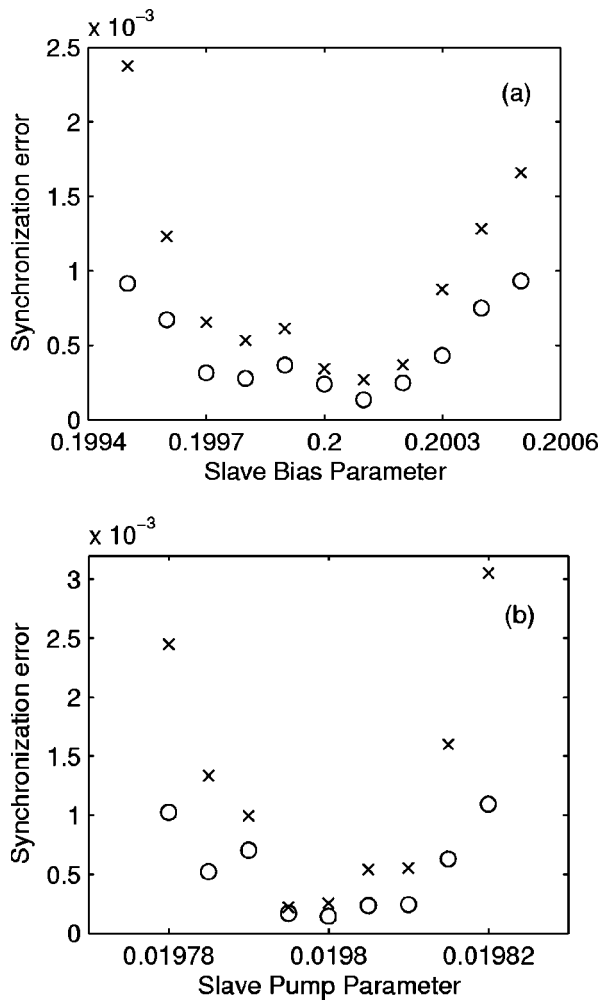
FIG. 10. Synchronization error, obtained from the numerical model, when considering different values of the slave bias and pump parameters. These parameters in the master laser have been fixed to 0.2 and 0.0198, respectively, and the coupling parameter $\epsilon=250$. (a) Mean value of the integrated error $e_T(34)$ (represented by circles) and 0.9 quantiles of $e_T(34)$ (represented by crosses), when the slave bias parameter takes different values from the master bias parameter. (b) Mean value of the integrated error $e_T(34)$ (represented by circles) and 0.9 quantiles of $e_T(34)$ (represented by crosses), when the slave pump parameter takes values which are different from the master pump parameter.
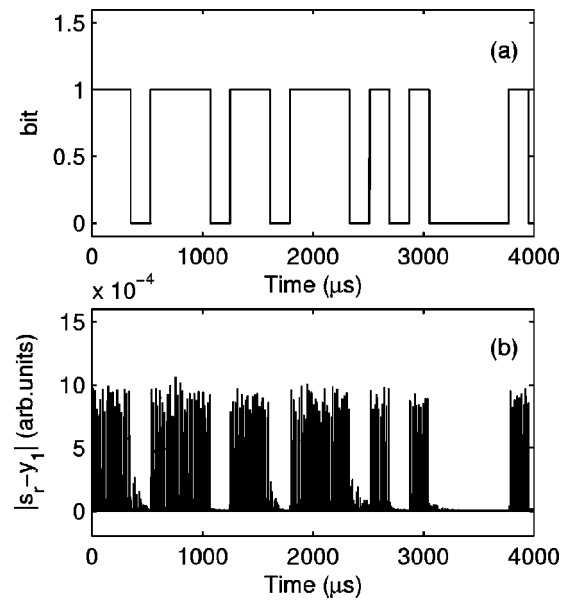

FIG. 12. Example of a communication scheme using the synchronization phenomenon between the master and the slave lasers. Numerical results. (a) Information message, represented by a sequence of bits "1" and "0"; each bit has a temporal duration of 180 μs. (b) Difference in absolute value between the received signal, s_r, and the slave intensity, y_1, when they are coupled with a coupling factor $\epsilon=250$.

adequate delay that compensates for the phase difference.

It turns out that, when the noise is not too high, during the transmission of a bit "0" the slave follows the dynamics of the master (synchronization), but during the transmission of a bit "1" there is no synchronization between master and slave. This can be seen in Fig. 12, where $\epsilon=250$. Figure 12(a) shows the message, as a temporal sequence of bits "1" and "0." The duration of each bit has been chosen equal to 18 spikes, that is, around 180 μs. Figure 12(b) is the difference in absolute value between the received signal, s_r, and the slave intensity, y_1. When the mean value of this difference during a bit is above (below) a certain threshold, a bit "1" ("0") is recovered.

In order to study the robustness of this simple communication scheme we have carried out a set of computer experiments corrupting the transmitted signal with an additive zero-mean white Gaussian noise component. Let us define the signal-to-noise ratio (SNR) as $10 \log_{10}(m_x^2/m_n^2)$ (dB), where m_x^2 and m_n^2 are the average signal power and the noise power, respectively. Figure 13 represents the bit error rate
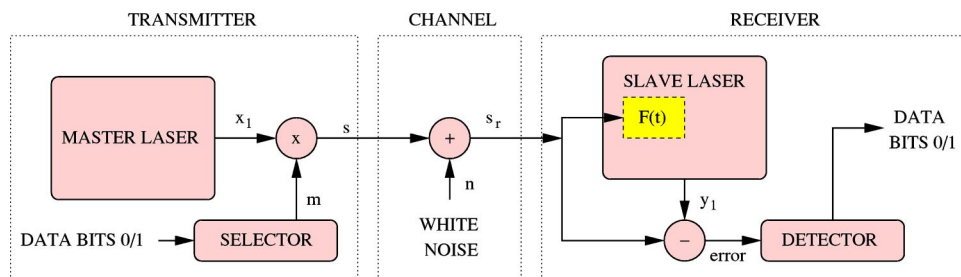

FIG. 11. Plot diagram of a digital communication system based on the master-slave configuration.
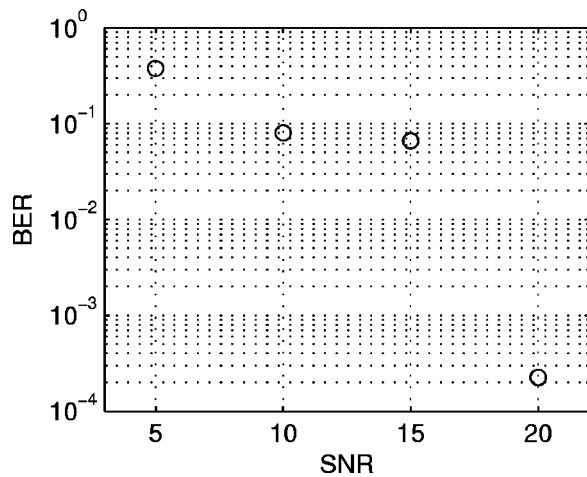
FIG. 13. BER for different values of the SNR. Numerical results.

(BER) attained by the system for different values of the SNR. We can see how for SNR=20, the BER is very close to 10^{-4}. In the simulations, the transmission of 10^5 bits has been considered for each value of the SNR. This number is sufficiently high, so the BER estimates are not affected by an increase of the number of simulations.

Additional applications of the proposed synchronization scheme potentially exist wherever nonlinear dynamical systems with external forcing can be used. One further example without leaving the field of digital communications is the problem of achieving synchronization with a chaotic carrier signal. Another area of potential application is control engineering, since the proposed coupling scheme can be viewed as an open-loop control system.

VI. CONCLUSIONS

We have introduced a scheme for coupling two nonautonomous, periodically forced, chaotic CO_2 lasers in a master-slave configuration in order to achieve complete synchronization. In this scheme, the forcing of the slave laser is introduced according to the difference between its intensity and that of the master. This way of coupling, that is, the modulation to the external forcing, is easy to implement in practice and can be applied not only to lasers but also to a broad class of periodically forced chaotic systems.

In this paper, experimental evidence of complete synchronization induced by a suitable coupling strength have been provided together with a detailed study of the synchronization properties by a numerical model that accurately reproduces the behavior of the physical system. In particular, we have calculated the conditional Lyapunov exponents as a function of the coupling strength, evaluated the time needed for synchronization, and also studied the robustness of the synchronization to parameter mismatches.

Finally, the proposed technique is applied to the design of a digital transmission system, the performance of which results to be satisfactory.

[1] L. M. Pecora and T. L. Carroll, Phys. Rev. Lett. **64**, 821 (1990).

[2] A. Pikovsky, M. Rosenblum, and J. Kurths, *Synchronization. A Universal Concept in Nonlinear Sciences* (Cambridge University Press, Cambridge, 2001).

[3] S. Boccaletti, J. Kurths, G. Osipov, D. L. Valladares, and C. S. Zhou, Phys. Rep. **366**, 1 (2002).

[4] C. Schäfer, M. G. Rosenblum, H.-H. Abel, and J. Kurths, Phys. Rev. E **60**, 857 (1999).

[5] B. Blasius, A. Huppert, and L. Stone, Nature (London) **399**, 354 (1999); S. Strogatz, *Sync: The Emerging Science of Spontaneous Order* (Hyperion, New York, 2003).

[6] K. Pyragas, Phys. Lett. A **181**, 203 (1993).

[7] L. Kocarev and U. Parlitz, Phys. Rev. Lett. **74**, 5028 (1995).

[8] P. Colet and R. Roy, Opt. Lett. **19**, 2056 (1994).

[9] M. G. Rosenblum, A. S. Pikovsky, and J. Kurths, Phys. Rev. Lett. **76**, 1804 (1996).

[10] N. F. Rulkov, M. M. Sushchik, L. S. Tsimring, and H. D. I. Abarbanel, Phys. Rev. E **51**, 980 (1995).

[11] L. Kocarev and U. Parlitz, Phys. Rev. Lett. **76**, 1816 (1996).

[12] E. M. Shahverdiev, S. Sivaprakasam, and K. A. Shore, Phys. Rev. E **66**, 037202 (2002).

[13] A. Murakami, Phys. Rev. E **65**, 056617 (2002); I. P. Mariño, E. Allaria, R. Meucci, S. Boccaletti, and F. T. Arecchi, Chaos **13**, 286 (2003).

[14] I. Bove, S. Boccaletti, J. Bragard, J. Kurths, and H. Mancini, Phys. Rev. E **69**, 016208 (2004).

[15] B. F. Kuntsevich and A. N. Pisarchik, Phys. Rev. E **64**, 046221 (2001).

[16] A. Uchida, T. Ogawa, M. Shinozuka, and F. Kannari, Phys. Rev. E **62**, 1960 (2000).

[17] K. Otsuka, R. Kawai, S. L. Hwong, J. Y. Ko, and J. L. Chern, Phys. Rev. Lett. **84**, 3049 (2000).

[18] E. G. Lariontsev, Opt. Express **2**, 198 (1998).

[19] V. Annovazzi-Lodi *et al.*, IEEE J. Quantum Electron. **32**, 953 (1996); A. Uchida *et al.*, Phys. Rev. E **65**, 066212 (2002).

[20] D. Y. Tang, R. Dykstra, M. W. Hamilton, and N. R. Heckenberg, Phys. Rev. E **57**, 3649 (1998).

[21] A. Uchida, R. McAllister, R. Meucci, and R. Roy, Phys. Rev. Lett. **91**, 174101 (2003).

[22] M. Ciofini, A. Labate, R. Meucci, and M. Galanti, Phys. Rev. E **60**, 398 (1999).

[23] C. Grebogi, E. Ott, and J. A. Yorke, Phys. Rev. Lett. **48**, 1507 (1992).

[24] B. Blasius and L. Stone, Int. J. Bifurcation Chaos Appl. Sci. Eng. **10**, 2361 (2000).

[25] R. Meucci, D. Cinotti, E. Allaria, I. Triandaf, L. Billings, I. B. Schwartz, and D. Morgan, Physica D **189**, 70 (2004).